Two-Stage Resource Allocation to Improve Utilization of Synchronous OFDM-PON Supporting Service Differentiation

Kyeong-Hwan Doo, Junseong Bang, Man Soo Han, Jonghyun Lee, and Sangsoo Lee

We propose a two-stage resource allocation algorithm for the high link utilization of an orthogonal frequency-division multiplexing passive optical network (OFDM-PON). An OFDM-PON is assumed to use a synchronous frame structure in supporting service differentiation. In distributing resources, the proposed algorithm first allocates a time window for each optical network unit (ONU), and then it arranges a subchannel, which is a group of subcarriers. This algorithm needs to satisfy two constraints. First, computations for the resource allocation should be done using a frame unit. Second, an ONU has to use a single subchannel to send upstream data for multiple services within a frame duration. We show through a computer simulation that the proposed algorithm improves the link utilization.

Keywords: OFDM-PON, resource allocation, service differentiation, synchronous frame, utilization.

I. Introduction

To provide bandwidth-intensive network services at low operation costs, a passive optical network (PON) needs to increase its transmission rate and coverage. For this reason, 10-gigabit-capable PON (XG-PON) and 10-gigabit Ethernet PON (10G-EPON) have been deployed for the past several years [1]. A time- and wavelength-division multiplexed PON (TWDM-PON) that combines the expansion of capacity by wavelength-division multiplexing (WDM) with stacked XG-PONs was chosen as a major solution for 40-gigabit-capable PONs (NG-PON2) [2]. It has been focused upon to provide a total of 40 Gbits/s on four downstream wavelengths (or 80 Gbits/s on eight wavelengths) and 2.5 Gbits/s or 10 Gbits/s on each of four upstream wavelengths (or each of eight wavelengths) [2]–[4]. Concurrently, as one of the post-NG-PON2 candidates, the orthogonal frequency-division multiplexing PON (OFDM-PON) has received a significant amount of attention over the past few years. The OFDM-PON increases both the transmission rate and distance of an optical network [5]. Moreover, the OFDM-PON, which is designed as a flexible architecture, can dynamically utilize its time and subcarriers [6].

For the efficient use of OFDM-PON's two-dimensional (2D) upstream resources (that is, time and subcarriers), several resource allocation algorithms have been proposed. In [7], under an OFDM-PON framework adapting a 10G-EPON MAC for a 2D frame structure, an algorithm that heuristically searches an optimal rectangle (that is, dimensions of a time window and subcarriers) providing a minimum upstream delay is proposed. In [8], under a similar framework with multiple

Manuscript received Aug. 4, 2014; revised Apr. 9, 2015; accepted May 8, 2015.

This work was supported by the ICT R&D program of MSIP/IITP, Rep. of Korea (14-000-05-002, Development of Key and Advanced Technologies for High-Capacity WDM Access Networks).

Kyeong-Hwan Doo (khdoo@etri.re.kr), Junseong Bang (hjbang21pp@etri.re.kr), Jonghyun Lee (jlee@etri.re.kr), and Sangsoo Lee (soolee@etri.re.kr) are with the Communications & Internet Research Laboratory, ETRI, Daejeon, Rep. of Korea.

Man Soo Han (corresponding author, mshan@mokpo.ac.kr) is with the Department of Information and Communications Engineering, Mokpo National University, Rep. of Korea.

subchannels (where a subchannel is a group of subcarriers), an Interleaved Polling with Adaptive Cycle Time–based 2D resource allocation algorithm is proposed to guarantee upstream delay performances of time-sensitive services. In [9], under a framework with time slots on multiple subchannels, upstream resource allocation algorithms based on shortest request first and greedy scheduling algorithms were studied.

An OFDM-PON has not been standardized yet. From conventional frameworks, most OFDM-PON allocation algorithms are based on a 10G-EPON framework. A 10G-EPON is different from an XG-PON. The first major difference is that a 10G-EPON is an asynchronous system, whereas an XG-PON is a synchronous system. Every operation of an XG-PON is synchronized with a frame duration fixed at 125 μs. In addition, a dynamic bandwidth allocation (DBA) operation is performed in every frame duration. On the other hand, a 10G-EPON has neither a fixed frame duration nor synchronization. The second major difference is that frame fragmentation is permitted in an XG-PON but not in a 10G-EPON. If the *grant size* is less than the size of a frame in a 10G-EPON, then the frame cannot be transmitted.

In this paper, we consider an OFDM-PON supporting service differentiation on a synchronous frame structure similar to an XG-PON. In Section II, we describe the synchronous OFDM-PON architecture with multiple subchannels. In addition, we present two constraints in designing an upstream resource allocation algorithm. In Section III, by maintaining the two constraints, we propose a two-stage upstream resource allocation algorithm (that is, a time window allocation stage and a subchannel reallocation stage) to increase the network utilization. In Section IV, the proposed algorithm is evaluated through computer simulations under balanced and unbalanced traffic distributions among optical network units (ONUs). Finally, Section V provides some concluding remarks regarding this proposal.

II. Synchronous OFDM-PON

1. Network Architecture

An OFDM-PON consists of an optical line terminal (OLT) and N ONUs in a point-to-multipoint topology [7]. The OFDM-PON has S subchannels, where a subchannel is a group of subcarriers. Each subchannel has the same number of subcarriers [8]. In this paper, different from the conventional OFDM-PON architectures described in [7]–[9], a synchronous OFDM-PON operates on a synchronous frame structure similar to that of an XG-PON, as shown in Fig. 1. It has a fixed frame duration of T_{FR}. We assume T_{FR} = 125 μs to take account

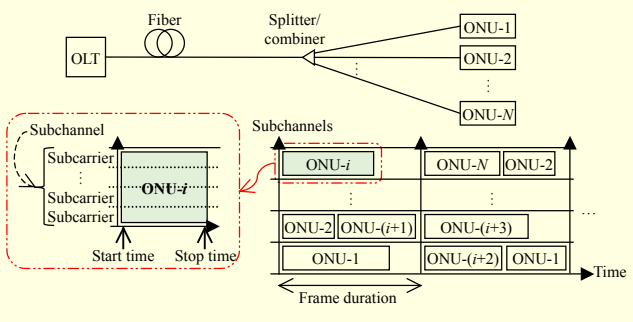

Fig. 1. Synchronous OFDM-PON architecture.

of the technical evolution from an XG-PON or a TWDM-PON. The OLT allocates a time window at a subchannel to each ONU. The time window is indicated by the start and stop times. The size of a time window in an upstream frame cannot exceed T_{FR}. The subchannel is indicated by a subchannel index (or by the start and end subcarrier indexes). Each ONU uses a subchannel at an allocated time window. In other words, subcarriers within a subchannel could not be shared among different ONUs at the same time. In terms of resource allocation, a subchannel in this paper is similar to a wavelength channel in a TWDM-PON with wavelength-tunable ONUs. In the earliest TWDM-PON, a stacked scheme independently uses a DBA method for each wavelength channel. However, in the latest papers on TWDM-PONs, the TWDM-PONs employ a joint DBA for all channels; a joint DBA arbitrates time and wavelength resources [10]–[12]. From this viewpoint, the presented scheme for the OFDM-PON of this paper can be compared with the TWDM-PON scheme.

A subchannel has N_{SC} subcarriers. In a subchannel, a *resource element* (RE) is an allocable space for an OFDM symbol, and a *resource block* (RB) is a set of REs for a symbol duration of T_{SB} (that is, 1 RB = N_{SC}·RE), and an OLT has multiple RBs, $S{\cdot}N_{RB}$, where N_{RB} is the number of RBs in a subchannel, as shown in Fig. 2. While the rectangle in [7] adapting an asynchronous system has a variable size in subcarrier and time dimensions, the RB as a minimum allocation unit has a fixed size to synchronize a frame. The throughput by the allocated RBs depends on the transmission efficiency of each ONU. The efficiency is increased by a high-order modulation format. Let m_i be the logarithmic value of a modulation format at ONU-i. For example, with the same RBs, the throughput with 16 quadrature amplitude modulation (16-QAM), $m_i = \log_2 16 = 4$, is twice that with 4-QAM; that is, $m_i = \log_2 4 = 2$. The modulation format is chosen based on the signal-to-noise ratio of each ONU, which is mainly affected by the fiber distance [13]. The maximum throughput at ONU-i is calculated by $m_i \times N_{RB}/T_{FR}$ (bits/s).

The Full Service Access Network group has defined

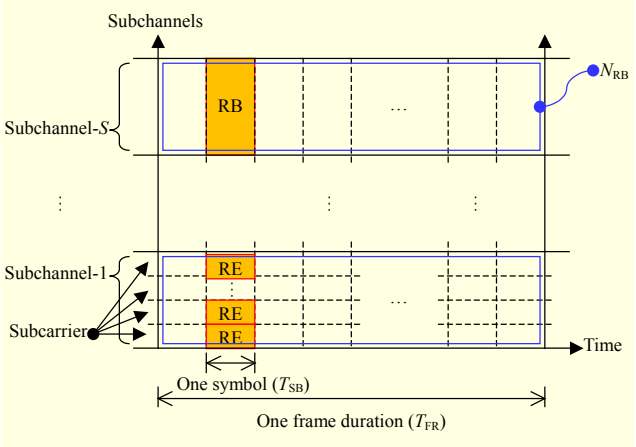

Fig. 2. Resource structure within frame.

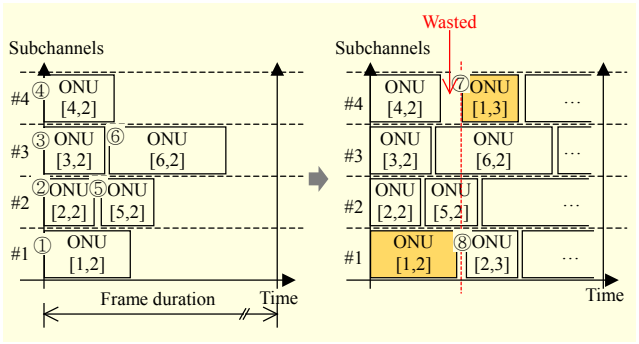

Fig. 3. Resource wasted by timing when sending differentiated upstream data.

five classes of service, called a transmission container (T-CONT), to provide QoS-aware traffic management in the XG-PON standard [14]. We suppose that a synchronous OFDM-PON also supports five T-CONT types that are identical with an XG-PON — T-CONT types 1 through 5. T-CONT type 1 is statically assigned and T-CONT type 5 is used for special purposes. Thus, we do not consider T-CONT types 1 and 5 in this paper. In other words, to focus on dynamically allocated resources [15], we only consider T-CONT types 2, 3, and 4. T-CONT type 2 supports an assured service. T-CONT type 3 includes assured and non-assured services. T-CONT type 4 supports a best-effort service. Each T-CONT type has a unique allocation identifier (AllocID) to identify a service type as well as an ONU.

2. Design Constraints for Resource Allocation

For resource allocation, an OLT transmits a 2D-bandwidth map (BWmap), which is conveyed by each downstream frame on the synchronous frame structure. The 2D-BWmap includes information for *grants* — a grant indicates the size of the time window and a subchannel index for the service type of each ONU. The 2D-BWmap needs to be computed in each frame. Each ONU determines how many RBs are allocated from the time window size and which subchannel is chosen from the subchannel index. An ONU sends its upstream data during a grant, with piggybacked queue length information (that is, *requests*) for multiple queues. Note that the modulation format for each ONU is already known to the OLT during the initialization process. If there is any change in the link, then an ONU will inform the OLT. In this polling, to generate a 2D-BWmap for resource allocation, the following two constraints should be satisfied for a synchronous OFDM-PON:

- *Constraint*-1: The 2D-BWmap has to be generated by computing the grants for all ONUs in every frame.
- *Constraint*-2: In each frame, an ONU has to use a single subchannel (that is, the same subcarriers) to send upstream data for grants to multiple services.

Constraint-1 is caused by a synchronous frame structure. To compute the grants for a large number of ONUs in each frame, a simple and routine allocation algorithm for hardware implementation has to be developed. Figure 3 illustrates an example of an ONU dynamically using several subchannels to send the upstream data corresponding to each grant (that is, a T-CONT type), to explain the necessity of *Constraint*-2. In this paper, ONU[i,j] denotes the T-CONT type-j of ONU-i. We assume that six ONUs are sequentially serviced from ONU-1 to ONU-6. The circled numbers (①–⑧) are the order of upstream resource use.

For load balancing, each T-CONT grant is to be assigned to a subchannel; the subchannel to be assigned is that which has the most available time at the moment of assignment, as shown in Fig. 3. An ONU cannot use multiple subchannels at the same time to send its upstream data. Thus, the data of ONU[1,3](⑦) cannot be transmitted until the data transmission of ONU[1,2](①) is completed, even though subchannel-#4 is available. This decreases the utilizations of the synchronous OFDM-PON. For these reasons, we need to keep *Constraint*-2.

III. Two-Stage Resource Allocation

A synchronous OFDM-PON needs to comply with both *Constraint*-1 and *Constraint*-2. We designed an allocation algorithm for hardware implementation in a synchronous OFDM-PON, and in this paper, we propose a two-stage upstream resource allocation algorithm to enhance a network's utilization rate: the first of the two stages is a time window allocation stage, and the second is a subchannel reallocation stage.

1. Time Window Allocation Stage

In the first stage, the RBs on an assigned subchannel under

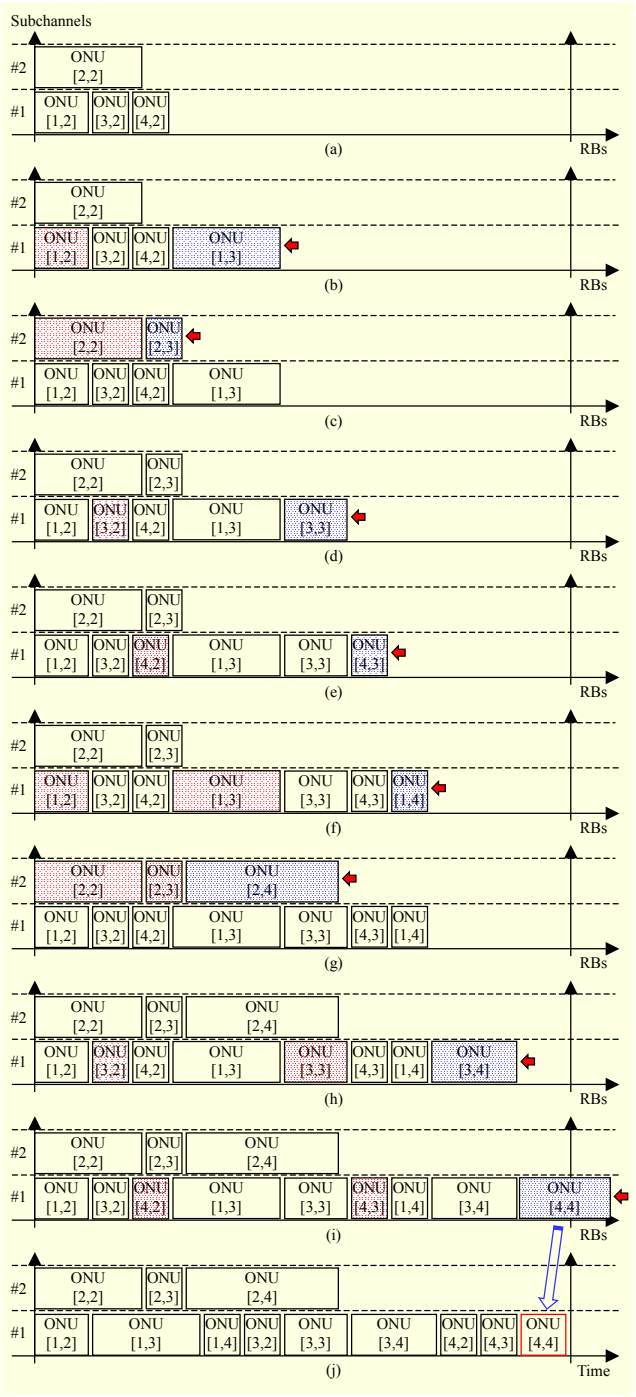

Fig. 4. Example of underutilization during time window allocation stage.

Constraint-2 are maximally allocated to each ONU in a greedy manner. We present an example of a time window allocation stage in Fig. 4. Four ONUs on two subchannels are serviced using T-CONT types 2, 3, and 4. This example shows the grant at each step for an allocation process that uses greedy allocation to differentiated services. The *x*-axis counts the number of RBs, with the exception of Fig. 4(j). The RBs between two bold arrows are allocable resources in an upstream frame. In Fig. 4(a), the RBs for T-CONT type-2 services of the four ONUs are sequentially reserved based on priority. In Figs. 4(b) through 4(e), a T-CONT type-3 service for each ONU is granted at the same subchannel, which is assigned in the step shown in Fig. 4(a) under *Constraint*-2. In Figs. 4(f) through 4(i), a T-CONT type-4 service for each ONU is granted in the same manner. In Fig. 4(j), the grants in a unit of the RBs are rearranged to generate a 2D-BWmap. As shown through *Constraint*-2, the network may be underutilized. In other words, this problem occurs because once an ONU chooses a subchannel for its upstream transmission in a frame, the ONU has to use the chosen subchannel for differentiated services. Under a balanced traffic distribution among ONUs, *Constraint*-2 is reasonable. However, under an unbalanced traffic distribution, network underutilization is induced, as shown in Fig. 4. Since the length of ONU[4,4] in Fig. 4 exceeds the frame duration of 125 μs, then only a partial amount is allocated, despite the fact that there is enough available space on subchannel-#2. That is, even though available space exists on other subchannels (that is, subchannel-#2 in Fig. 4 in this case), ONU[4,4] could not take the necessary resources it needed.

To overcome this problem, we propose a two-stage upstream resource allocation algorithm; that is, a time window allocation stage and a subchannel reallocation stage. In the first stage, a time window is allocated on a temporarily assigned subchannel to each grant. In the second stage, the temporary subchannel will be replaced with a confirmed subchannel. We next describe the operations for a time window allocation. In terms of the code reuse, the allocation processes for a T-CONT type are similar to each other. The pseudocode is presented in Algorithms 1 and 2. Let *alloc_id*(i,j) return an AllocID of a queue for a T-CONT type-j of an ONU-i. We present the following two service parameters for each queue with *alloc_id*(i,j):

- *MSI*(k) is a maximum service interval for a queue having AllocID of k (that is, *alloc_id*(i,j) = k), where an interval is represented in the unit of 125 μs.
- *MSB*(k) is the maximum number of RBs that can be allocated to a queue having AllocID of k during *MSI*(k). This value depends on the transmission efficiency; that is, m_i. In other words, for the same throughput, the number of RBs for an ONU with 4-QAM is twice that for an ONU with 16-QAM.

Algorithm 1. Time window allocation.

```
1:  i = stop = rr_pointer(j); // j=2,3,4 for T-CONT type
2:  while(true){
3:      v = W(i);
4:      if (W(i) = 0){
```

```
5:          W_tmp(i) = index_of_max(FB(1), ... , FB(S));
6:          v = W_tmp(i);
7:        }
8:        k = alloc_id(i,j);
9:        if (request(k) > 0 and BC(k) > 0) {
10:         grant(k)=min(BC(k), request(k), FB(v));
11:         BC(k) = BC(k) – grant(k);
12:         request(k) = request(k) – grant(k);
13:         FB(v) = FB(v) – grant(k);
14:         if (grant(k) > 0 and W(i) = 0) W(i) = W_tmp(i);
15:       }
16:       do the subchannel reallocation stage for ONU-i;
17:       i++;
18:       if (i = N) i = 0;
19:       if (i = stop) break;
20:   }
```

We use the following variables for a two-stage upstream resource allocation:

- $IC(k)$ is an interval counter. After $IC(k)$ is initially set to the maximum service interval (that is, $MSI(k)$), it is decreased by one for every frame. If it is expired (that is, $IC(k) = 1$), then it is reset to $MSI(k)$ for the next frame.
- $BC(k)$ is an RB counter. It denotes the remaining RBs of a queue having AllocID of k during $IC(k)$. When $IC(k) = 1$, $BC(k)$ is reset to $MSB(k)$ for the next frame.
- $FB(v)$ is the remaining (that is, allocable) RBs at an upstream subchannel v in a given frame. $RB(v)$ is initiated to the maximum value at the beginning of the allocation process.
- $W(i)$ is an index of an upstream subchannel allocated to an ONU-i, $i = 0, \dots, N–1$. In each frame, initially $W(i) = 0$; that is, no subchannel is allocated to an ONU-i. If ONU-i uses a subchannel v, $v = 1, \dots, S$, then $W(i) = v$.
- $W\_tmp(i)$ is a temporary index of an upstream subchannel for searching $W(i)$. If $W(i) = 0$, then $W\_tmp(i)$ will be assigned by the index of the maximum $FB(v)$.
- *rr_pointer*(j) is a round-robin pointer, which indicates the starting ONU number for each allocation process.
- *index_of_max*(…) returns an index of the maximum variable among inputs. For example, if $FB(3)$ is the maximum, then *index_of_max*($FB(1), FB(2), FB(3)$) = 3.
- *request*(k) is the requested RBs with $k = alloc\_id(i,j)$.
- *grant*(k) is the granted RBs with $k = alloc\_id(i,j)$.
- $GB(i)$ is the sum of granted RBs for an ONU-i.

In the case of a synchronous OFDM-PON, the latency requirement on a service-level agreement (SLA) is satisfied with $MSI(k)$. For example, if $MSI(k)$ is 3, then it should be granted more than once within three frames. A service rate for a T-CONT type of an ONU is obtained as $m_i \times grant(k)/(MSI(k) \times T_{FR})$ bits/s. And, the maximum service rate is expressed as $m_i \times MSB(k)/(MSI(k) \times T_{FR})$ bits/s.

The allocation process starts with T-CONT type 2. The process will then be repeated with T-CONT types 3 and 4. In other words, the priority order is T-CONT type 2, 3, and 4. In Algorithm 1, the start index for ONU-i is indicated by *rr_pointer*(j), where T-CONT type-j is 2, 3, and 4. In lines 3 through 7, if a subchannel index v loaded from $W(i)$ is already set in the range of 1 to S, then the same subchannel will be used for upstream data under *Constraint*-2. Otherwise, that is, $W(i) = 0$, the subchannel that has the most remaining RBs will then be initially assigned to ONU-i. In line 8, an AllocID for T-CONT type-j of ONU-i is returned by $alloc\_id(i,j)$ to k. After checking the allocation availability in line 9, the RBs are granted to ONU-i. In line 10, $grant(k)$ is the minimum of $BC(k)$, $request(k)$, and $FB(v)$, where $v = W(i)$ if $W(i) > 0$; otherwise, $v = W\_tmp(i)$. Then, $BC(k)$, $request(k)$, and $FB(v)$ are decreased by $grant(k)$. When $grant(k) > 0$ and $W(i) = 0$, $W(i)$ is substituted by $W\_tmp(i)$. After the time window allocation for ONU-i, the next stage (that is, the subchannel reallocation stage) will be conducted. This process is repeated by increasing index i under the conditions in lines 18 and 19. When this process is stopped, the value of the current index i is stored in *rr_pointer*(j), increasing by 1 to provide service fairness among the ONUs. The subchannel reallocation stage for ONU-i in line 16 of Algorithm 1 will be explained in the next paragraph.

2. Subchannel Reallocation Stage

In the second stage, a subchannel is reallocated to ONU-i, by swapping the new subchannel and temporarily assigned subchannel.

Algorithm 2. Subchannel reallocation.

```
1:    v = W(i);
2:    if (v > 0){
3:      u = index_of_max(FB(1) – GB(i), … ,
4:            FB(v), … , FB(S) – GB(i));
5:      if (u≠v){
6:        FB(v) = FB(v) + GB(i);
7:        FB(u) = FB(u) – GB(i);
8:        W(i) = u;
9:      }
10:   }
```

This swapping algorithm avoids the underutilization (for example, Fig. 4) that occurs by *Constraint*-2. To avoid an inefficient subchannel allocation, we reallocate the upstream subchannel after the grant operation. The pseudocode for the subchannel reallocation stage is presented in Algorithm 2.

The basic principle is to minimize the remaining RBs to increase the network utilization. This is obtained by *index_of_max*($FB(1) – GB(i), \dots, FB(v–1) – GB(i), FB(v), \dots,$

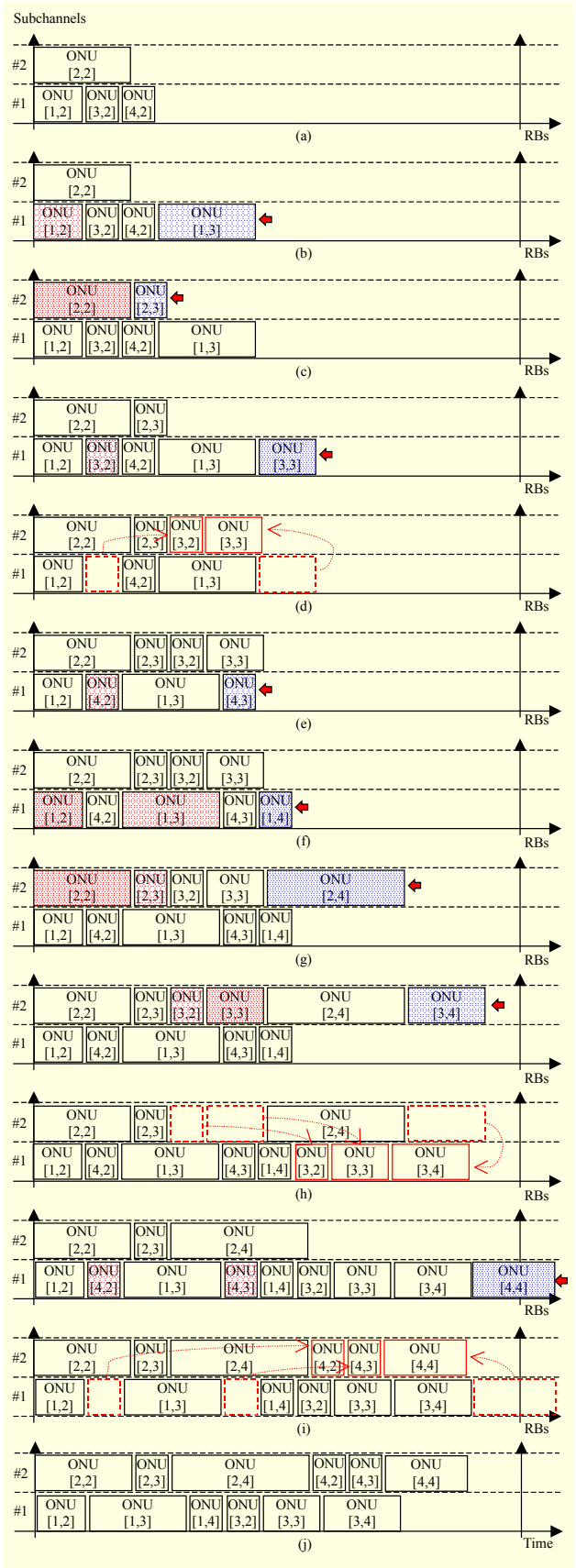

Fig. 5. Example of two-stage resource allocation algorithm.

$FB(v+1) - GB(i), \ldots, FB(S) - GB(i)$). If temporary value u is not equal to index v, then subchannel v for the granted RBs is changed to u, as shown in lines 6 through 8 in Algorithm 2.

We illustrate an example of our two-stage upstream resource allocation algorithm in Fig. 5. To visually compare the final results, four ONUs with three T-CONT types on two subchannels are assumed. Figures 5(a) through 5(c) are the same as Figs. 4(a) through 4(c). In Fig. 5(d), through the second stage, ONU[3,2] and ONU[3,3] are moved from subchannel-#1 to subchannel-#2 to balance the loads between the two subchannels. In Figs. 5(e) through 5(i), each subchannel for the ONU grants are rearranged in the same manner. In Fig. 5(j), ONU[4,4] could take the necessary resources it needs. We visually show the expected results of the proposed algorithm in Fig. 5(j), which is compared with Fig. 4(j).

IV. Results and Discussion

For an OFDM-PON, we evaluated the delay performances of the proposed algorithm under balanced and unbalanced traffic distribution among the ONUs. We label two systems as System-A and System-B. System-A consists of four separated XG-PON systems. At each wavelength providing an upstream of 2.5 Gbits/s, eight ONUs are initially serviced at nearly 400 Mbits/s. The wavelengths are compared with the subchannels for the OFDM-PON. The transmission distance between an OLT and each ONU is assumed to be 20 km, and the ONU response time is 35 μs [15]. Each queue size for a T-CONT type is assumed to be 1 Mbytes. The proposed algorithm can be applied by fixing $W(i)$ to a system such as that of System-A with four upstream wavelengths. System-B is an OFDM-PON with four upstream subchannels for 32 ONUs. In [16]–[17], the OFDM symbol length is set to 1.28 ns, 2.56 ns, or 5.12 ns. In [18], a symbol length of 12.8 ns is used for an FPGA-based system test. We use 12.8 ns for the symbol length. Each subchannel consists of 16 subcarriers and has 19,440 RBs with 4 QAM. The bandwidth of each upstream subchannel is 2.5 Gbits/s. The other parameters are the same as those of System-A. System-B uses a two-stage resource allocation algorithm. To compare with System-A, for T-CONT type 2 of System-B, we set $MSB(k)$ = 7,810 RBs (15,620 bytes for System-A) and $MSI(k)$ = 5 for 200 Mbits/s. For both T-CONT types 3 and 4, we set $MSB(k)$ = 15,620 RBs (31,240 bytes for System-A) and $MSI(k)$ = 10 for 200 Mbits/s. The initial value of $FB(v)$ is 19,440 RBs (approximately 38,880 bytes for System-A) for all v. For the input traffic to an ONU, we consider a self-similar traffic model generated by many Pareto-distributed on-off processes. The two shape parameters for the on and off intervals are set to 1.4 and 1.2, respectively. We use

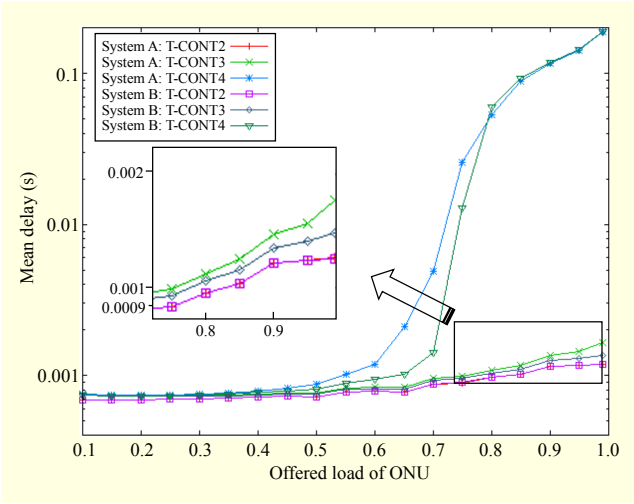

Fig. 6. Mean delay under balanced traffic distribution.

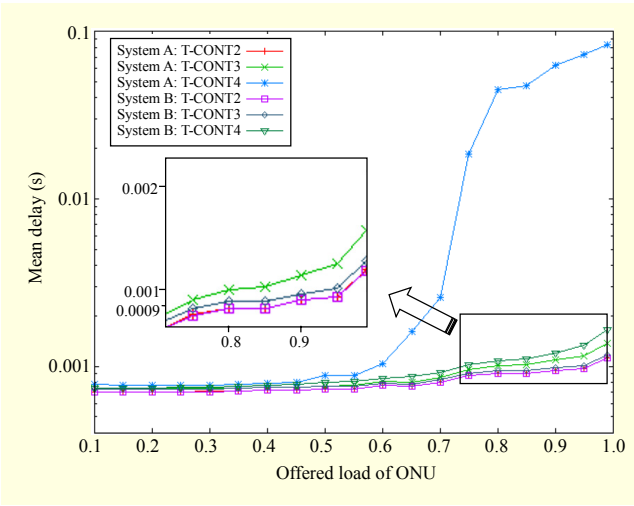

Fig. 7. Mean delay under unbalanced traffic distribution.

a tri-modal-based frame size distribution, in which the frame sizes are 64 bytes, 500 bytes, and 1,500 bytes, and their load fractions are 60%, 20%, and 20%, respectively, as in [15]. We assume that the load fractions of T-CONT types 2, 3, and 4 of each ONU are 35%, 35%, and 30%, respectively. For each plot point, the simulation is performed until the total number of frames transmitted to the OLT exceeds 10^9 for each system.

We consider a balanced traffic scenario in which each ONU has an identical input load and an unbalanced traffic scenario, which is more practical to evaluate both systems. The unbalanced traffic scenario is assumed as follows. In System-A, the offered load rate of each ONU of the two wavelengths is fixed at 0.4. In System-B, the offered load rate of ONU-i is fixed at 0.4, where $i = 0, \ldots, 15$. The offered load rate of the other ONUs in both systems is increased from 0.1 to 0.99. The offered load rate means input traffic rate per maximum rate

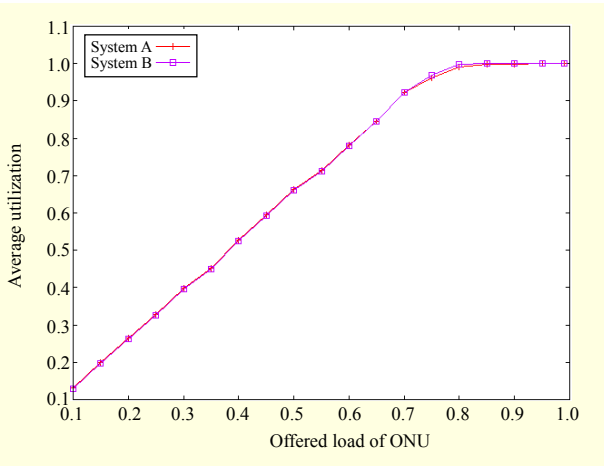

Fig. 8. Average utilization under balanced traffic distribution.

(400 Mbits/s) into each ONU.

The simulation results are shown in Figs. 6 through 9. Figures 6 and 7 illustrate, respectively, the mean delays under a balanced and an unbalanced traffic distribution for both System-A and System-B. The mean delay increases as the offered load rate of an ONU increases. There is little difference between the two systems for T-CONT type 2, which is an assured service.

The mean delay of System-B is improved by up to 20% for T-CONT type 3 compared to that of System-A, under both traffic distributions. On the other hand, for T-CONT type 4, it is dramatically improved thanks to the dynamic subchannel reallocation of System-B under an unbalanced traffic distribution. The unused bandwidth of ONUs having a fixed load rate is utilized by other ONUs in System-B, whereas this kind of utilization is difficult in System-A.

Figures 8 and 9 illustrate, respectively, the average utilization under a balanced and an unbalanced traffic distribution for both systems. The average utilization is a used upstream bandwidth per total available bandwidth during simulation duration. There is little difference of mean utilization between the two systems under a balanced traffic distribution, as shown in Fig. 8. The average utilization of System-B is much improved under an unbalanced traffic distribution over 0.75 of the offered load of an ONU, as shown in Fig. 9. Subchannel reallocation under an unbalanced traffic distribution has a significant effect on the average utilization because the requested amount among each subchannel is dynamically changed.

In Fig. 10, we present functional block diagrams of an OLT and an ONU MAC for implementation with four upstream subchannels. The transmission rate of an OLT MAC is symmetric at 10 Gbits/s, through each subchannel is 2.5 Gbits/s, and that of an ONU MAC is asymmetric at 10/2.5 Gbits/s.

Figure 11 illustrates real-time VHDL functional simulation

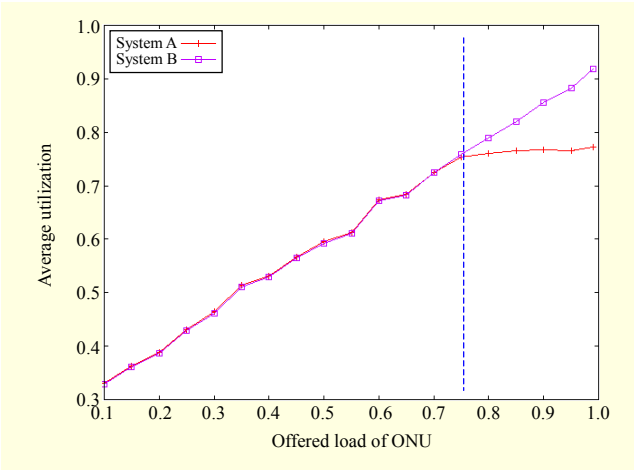

Fig. 9. Average utilization under unbalanced traffic distribution.

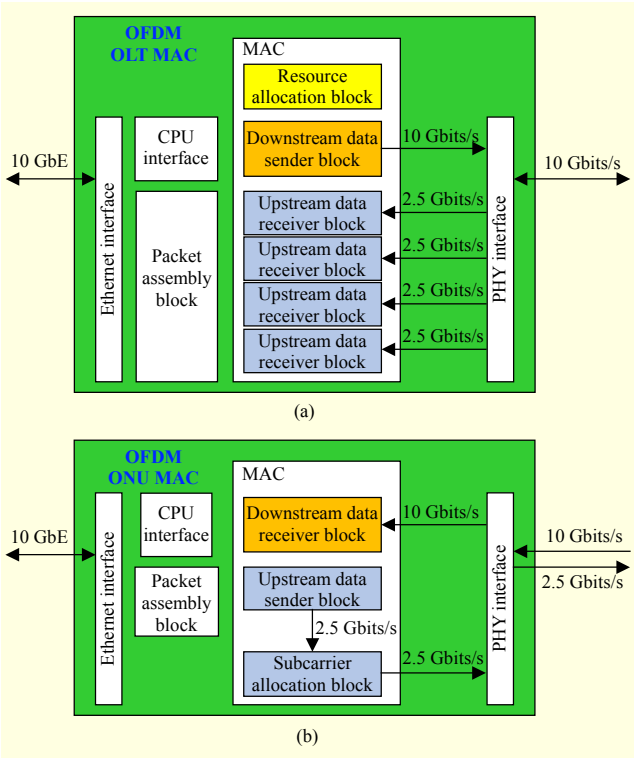

Fig. 10. Functional block diagrams for (a) OLT MAC and (b) ONU MAC.

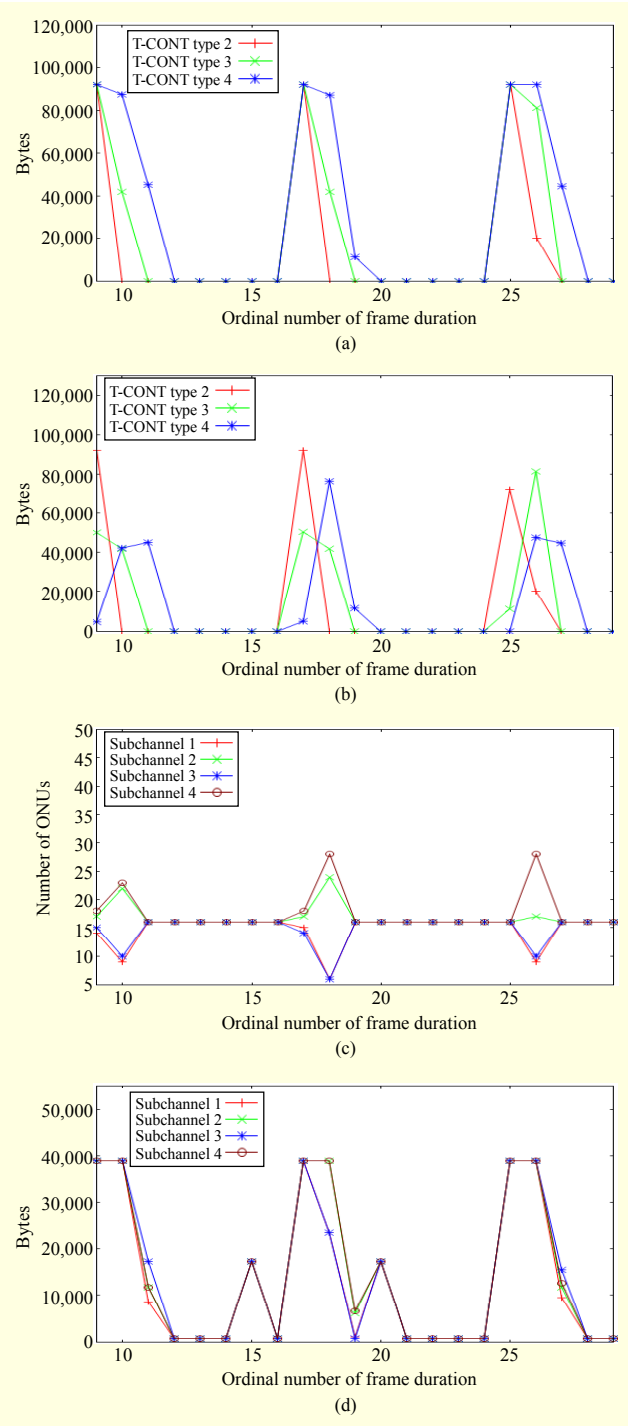

Fig. 11. Real-time functional simulation results: (a) request of T-CONT types, (b) grant of T-CONT types, (c) number of ONUs at each subchannel, and (d) allocated frame bytes at each subchannel.

results plotted by a gnuplot graph. In Fig. 11, the frame duration on the *x*-axis is increased at an interval of 125 μs; the *y*-axis in (a), (b), and (d) indicates the sum of the bytes used in the four subchannels during a frame duration; and the *y*-axis in (c) is the number of ONUs assigned to each subchannel.

When request (a) is more than grant (b), T-CONT type 2 is assured in accordance with priorities, whereas T-CONT types 3 and 4 are granted as much as is permitted. Even though the number of ONUs assigned to each subchannel (c) is different, frame bytes allocated to each subchannel (d) are normalized at about 38,880 bytes by the subchannel reallocation stage, as shown at the 10th frame duration in (c) and (d).

V. Conclusion

For a synchronous OFDM-PON, we proposed a two-stage resource allocation algorithm consisting of a time window allocation stage and a subchannel reallocation stage. In the first stage, the available upstream time resources were allocated to ONUs in a greedy manner. In the second stage, a subchannel was assigned to an ONU suffering from an unbalanced traffic distribution among subchannels. An assigned subchannel was rearranged to enhance network utilization. Our proposed algorithm was evaluated through computer simulations under balanced and unbalanced traffic environments. The utilization was improved by up to 20% for T-CONT type 3. For T-CONT type 4, the overall performance was dramatically improved under a heavily unbalanced traffic load of over 0.75.

References

[1] J. Kim, H. Bang, and C.-S. Park, "Design and Performance Analysis of Passively Extended XG-PON with CWDM Upstream," *J. Lightw. Technol.*, vol. 30, no. 11, June 2012, pp. 1677–1684.

[2] ITU-T Rec. G.989 Series Draft Version, *40-Gigabit-Capable Passive Optical Networks (NG-PON2)*, Mar. 2013.

[3] Y. Luo et al., "Time- and Wavelength-Division Multiplexed Passive Optical Network (TWDM-PON) for Next-Generation PON Stage 2 (NG-PON2)," *J. Lightw. Technol.*, vol. 31, no. 4, Feb. 2013, pp. 587–593.

[4] A. Dixit et al., "Dynamic Bandwidth Allocation with Optimal Wavelength Switching in TWDM-PONs," *Int. Conf. Transparent Opt. Netw.*, Cartagena, Spain, June 23–27, 2013, pp. 1–4.

[5] N. Cvijetic, D. Qian, and J. Hu, "100 Gb/s Optical Access Based on Optical Orthogonal Frequency-Division Multiplexing," *IEEE Commun. Mag.*, vol. 48, no. 7, July 2010, pp. 70–77.

[6] N. Cvijetic, "OFDM for Next-Generation Optical Access Networks," *J. Lightw. Technol.*, vol. 30, no. 4, Feb. 2012, pp. 384–398.

[7] K. Kanonakis, E. Giacoumidis, and I. Tomkos, "Physical-Layer-Aware MAC Schemes for Dynamic Subcarrier Assignment in OFDMA-PON Networks," *J. Lightw. Technol.*, vol. 30, no. 12, June 2012, pp. 1915–1923.

[8] H. Bang et al., "Design and Analysis of IPACT-Based Bandwidth Allocation for Delay Guarantee in OFDMA-PON," *J. Opt. Commun. Netw.*, vol. 5, no. 11, Nov. 2013, pp. 1236–1249.

[9] M. Bi, S. Xiao, and L. Wang, "Joint Subcarrier Channel and Time Slots Allocation Algorithm in OFDMA Passive Optical Networks," *Optics Commun.*, vol. 287, Jan. 15, 2013, pp. 90–95.

[10] A.R. Dhaini et al., "Dynamic Wavelength and Bandwidth Allocation in Hybrid TDM/WDM EPON Networks," *J. Lightw. Technol.*, vol. 25, no. 1, Jan. 2007, pp. 277–286.

[11] M.P. McGarry et al., "Just-in-Time Scheduling for Multichannel EPONs," *J. Lightw. Technol.*, vol. 26, no. 10, May 2008, pp. 1204–1216.

[12] K. Kanonakis and I. Tomkos, "Improving the Efficiency of Online Upstream Scheduling and Wavelength Assignment in Hybrid WDM/TDMA EPON Networks," *IEEE J. Sel. Areas Commun.*, vol. 28, no. 6, Aug. 2010, pp. 838–848.

[13] C.H. Yeh et al., "Using Adaptive Four-Band OFDM Modulation with 40 Gb/s Downstream and 10 Gb/s Upstream Signals for Next Generation Long-Reach PON," *Opt. Exp.*, vol. 19, no. 27, Dec. 2011, pp. 26150–26160.

[14] ITU-T Rec. G.987.3, *10-Gigabit-Capable Passive Optical Networks (XG-PON): Transmission Convergence (TC) Layer Specification*, Jan. 2014.

[15] M.S. Han, H. Yoo, and D.S. Lee, "Development of Efficient Dynamic Bandwidth Allocation Algorithm for XGPON," *ETRI J.*, vol. 35, no. 1, Feb. 2013, pp. 18–26.

[16] E.F. Mateo, X. Zhou, and G. Li, "Selective Post-Compensation of Nonlinear Impairments in Polarization-Division Multiplexed WDM Systems with Different Channel Granularities," *IEEE J. Quantum Electron.*, vol. 47, no. 1, Jan. 2011, pp. 109–116.

[17] P. Medina, V. Almenar, and J.L. Corral, "Evaluation of Optical ZP-OFDM Transmission Performance in Multimode Fiber Links," *Opt. Exp.*, vol. 22, no. 1, Jan. 13, 2014, pp. 1008–1017.

[18] M. Dreschmann et al., "An Ultra-high Speed OFDMA System for Optical Access Networks," *Int. Conf. Comput., Netw. Commun.*, Honolulu, HI, USA, Feb. 3–6, 2014, pp. 889–894.

Kyeong-Hwan Doo received his BS and MS degrees in electronic engineering from Chonbuk National University, Jeonju, Rep. of Korea, in 1996 and 1998, respectively, and his PhD degree in electronic engineering from Chungnam National University, Daejeon, Rep. of Korea, in 2013. In 2000, he joined the Electronics and Telecommunications Research Institute, Daejeon, Rep. of Korea. His research interest includes scheduling in high-speed networks, passive optical networks, and optical OFDM.

Junseong Bang received his BS degree in computer science and engineering from Hanyang University, Ansan, Rep. of Korea, in 2006 and his MS and PhD degrees in information and communications from Gwangju Institute of Science and Technology, Rep. of Korea, in 2009 and 2013, respectively. Since 2013, he has been with the Electronics and Telecommunications Research Institute, Daejeon, Rep. of Korea. His main research interests are algorithms; system optimization; integrated optical and wireless networks; and mobile ad hoc networks.

Man Soo Han received his BS, MS, and PhD degrees in electrical engineering from the Korea Advanced Institute of Science and Technology, Daejeon, Rep. of Korea, in 1992, 1994, and 1999, respectively. He was a senior researcher at the Electronics and Telecommunications Research Institute, Daejeon, Rep. of Korea from 1999 to 2003. Currently, he is a professor with the Department of Information and Communications Engineering, Mokpo National University, Rep. of Korea. His research interests include scheduling in high-speed networks, passive optical networks, and wireless networks.

Jonghyun Lee received his BS and MS degrees in electronic engineering from Sungkyunkwan University, Suwon, Rep. of Korea, in 1981 and 1983, respectively. He received his PhD degree in communication engineering from the same university in 1993. In 1983, he joined the Electronics and Telecommunications Research Institute (ETRI), Daejeon, Rep. of Korea. His current research activities include optical communication systems and optical internet technology. He is currently the head of the Optical Internet Research Department of ETRI.

Sangsoo Lee received his BS and MS degrees in applied physics from Inha University, Incheon, Rep. of Korea, in 1988 and 1990, respectively. He received his PhD degree in the area of DWDM transmission technology from the same university in 2001. In 1990, he joined the Electronics and Telecommunications Research Institute (ETRI), Daejeon, Rep. of Korea. His current research interests include optical access networks, WDM-PON, and energy-efficient network technology. He is the head of the Optical Access Research Team of ETRI.